2025 IMEKO TC26 International Conference on
Metrology for Archaeology and Cultural Heritage
Bergamo, Italy, October 15-17, 2025

Infrared and Terahertz Imaging for the Analysis of a Fresco Sample

Emma Vannini[1,2], Ilaria Catapano[3], Alice Dal Fovo[1], Valentina Di Sarno[4], Alessandra Rocco[4], Pasquale Maddaloni[4], and Raffaella Fontana[1]

[1] National Research Council – National Institute of Optics (CNR-INO), Largo E. Fermi 6, 50125 Firenze, Italy; emma.vannini@ino.cnr.it, alice.dalfovo@ino.cnr.it, raffaella.fontana@ino.cnr.it
[2]Department of Physics and Astronomy, University of Florence, Via Sansone 1, 50019 Sesto Fiorentino (FI), Italy; emma.vannini@unifi.it
[3] National Research Council – Institute for Electromagnetic Sensing of the Environment (CNR-IREA), Via Diocleziano 328, 80124 Naples, Italy; catapano.i@irea.cnr.it
[4] National Research Council – National Institute of Optics (CNR-INO), Via Campi Flegrei 34, 80078 Pozzuoli (NA), Italy; valentina.disarno@ino.cnr.it; alessandra.rocco@ino.cnr.it; pasquale.maddaloni@ino.cnr.it

***Abstract* – The stratigraphy of mural paintings comprises multiple plaster layers with varying thicknesses, each prepared with progressively finer sand. Due to this complex structure, wall paintings are susceptible to deterioration at different depths. Detecting subsurface and internal defects, as well as hidden features, is crucial in conservation to reveal underlying details and assess the artwork's condition. Infrared (IR) and terahertz (THz) radiation can penetrate beneath the surface, providing valuable diagnostic insights. In this work, a multi-technique survey was performed on a purpose-built sample using Near-Infrared (NIR) reflectography, active thermography in both Mid-Wave (MWIR) and Long-Wave Infrared (LWIR) ranges, and Terahertz Time-Domain Imaging (THz-TDI). The results demonstrate the capabilities and limits of these techniques in identifying subsurface features and highlight their complementary roles in the analysis and conservation of wall paintings.**

I. INTRODUCTION

Mural paintings vary in form depending on the artistic technique employed. Traditional murals typically consist of multiple plaster layers, composed of slaked lime mixed with sand of varying grain sizes. The stratigraphy includes layers of different thicknesses, from the thick *arriccio* to the fine *intonachino*, each prepared with progressively finer sand to achieve a smooth surface suitable for pigment application.

Due to this complex, multilayered structure, wall paintings are prone to deterioration, affecting both superficial and subsurface layers. Common degradation phenomena include the detachment of painted areas, surface salt crystallisation, superficial discontinuities, and micro-fractures, as well as deeper defects such as air gaps and cracks, often caused by fluctuations in temperature and humidity. Furthermore, historical murals sometimes conceal earlier artworks beneath layers of white or pigmented slaked lime, applied either during restoration or to prepare a new painting surface.

The penetration capabilities of infrared radiation make Near-Infrared (NIR) reflectography and active thermography in the Mid-Wave (MWIR) and Long-Wave Infrared (LWIR) ranges effective non-invasive methods for investigating subsurface features in mural paintings [1–5]. In the last ten years, reflection-mode Terahertz (THz) imaging has demonstrated considerable potential in wall painting analysis, proving highly sensitive in revealing hidden features and further establishing its value in cultural heritage diagnostics [6-8].

This work presents a diagnostic campaign aimed at evaluating the combined use of these techniques and assessing their individual contributions to detecting hidden elements in murals [9,10]. To this end, a sample simulating typical fresco stratigraphy, including concealed decorations, was prepared and analysed. We employed four instruments: a multi-spectral scanner operating in the Visible-NIR range (395 – 2550 nm), two thermal cameras covering the MWIR (3 – 5 μm) and LWIR (8 – 14 μm) ranges, and a THz spectrometer.

II. MATERIALS

The analysed sample was specially prepared by a professional art conservator. The object consists of a terracotta slab (35 × 45 cm^2) divided into nine sections (7 × 11 cm^2 each), arranged in three rows to simulate mural painting stratigraphy and replicate hidden decorative elements (Fig. 1). The sample was fabricated following the traditional fresco technique. Consequently, the composition and materials of the plaster layers, including pigments and metals, were selected based on the historical

relevance to frescoes, adhering to ancient recipes and execution protocols followed by master painters.

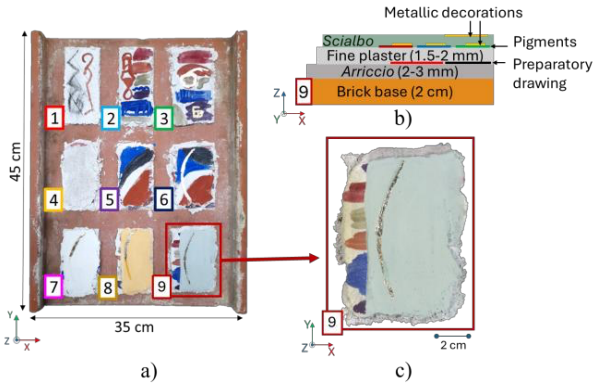

Fig. 1. a) Terracotta slab subdivided into nine distinct areas; b) schematic cross-sectional representation of area 9; c) detailed magnification of area 9.

Each section begins with an *arriccio* base layer. On top of this, preparatory drawings were created using iron oxide and carbon black pigments. These remain fully visible in area 1, representing the most used materials for transferring compositional designs onto the wall prior to pigment application. In areas 2-9, a painted plaster layer was applied on top of the *arriccio* using the fresco technique (exemplified in area 2). Further embellishments, simulating the typical gilding of haloes and decorative elements, were incorporated in area 3 using gold and silver leaf applied via the oil (or mordant) gilding technique, which was the most common method for affixing metal leaf onto mural surfaces.

The second row replicates the historical practice of overlaying an existing painting with a new plaster layer. This overlying layer was left unpainted in area 4, painted in area 5, and decorated with metallic leaf in area 6.

The third row considers the presence of *scialbatura*, a traditional technique used to conceal underlying paintings with a thin lime wash. Here, coloured lime washes, mixed with starch tempera and fine-grained pigments, were applied in white (area 7), yellow (area 8), and green (area 9) to replicate some of the most prevalent varieties of *scialbatura* found in fresco paintings, both in terms of chromatic characteristics and binding medium

III. METHODS

A. Vis-NIR Reflectance Imaging Spectroscopy (RIS)

The visible and near-infrared spectral ranges were investigated using a multispectral scanner developed by the Heritage Science group at CNR-INO [11]. This system integrates pointwise spectral information (395-2550 nm) with whiskbroom scanning. Backscattered light is collected and directed to silicon (Si, 395-950 nm) and indium gallium arsenide (InGaAs, 1050-2550 nm) photodiodes, each coupled with an interferential filter for wavelength selection. The spectral resolution is 20–30 nm in the visible range and 66–120 nm in the NIR range. A 45°/0° illumination/detection geometry was employed, with the scanner head moving across the surface via an XY translation stage (250 µm sampling step, 500 mm/s speed), enabling a 1 m^2 scan in 3 hours. An autofocus system maintains optical alignment during acquisition.

The output comprises 32 co-registered monochromatic images (16 visible, 16 NIR), forming a metrically accurate RIS data cube. These data permit both single-wavelength image analysis and spectral profiling at user-defined points.

The sample was scanned in a single acquisition covering an area of 26.7 × 41.7 cm^2.

B. MWIR Active Thermography

Mid-wave-infrared analysis was performed using a FLIR A6751 MWIR thermal camera with an indium antimonide (InSb) detector (3–5 µm, operational range: -20 °C to 50 °C). The detector (640 × 512 pixels, 15 µm pitch) achieves a Noise Equivalent Temperature Difference (NETD) < 20 mK and ± 2 °C accuracy (-20 °C to 350 °C), operating up to 480 fps (ResearchIR MAX software).

Two symmetrically positioned 1 kW halogen lamps (~100 cm sample distance) provided uniform illumination. The sample was heated for 180 s, followed by cooling-phase recording (1 fps) until thermal equilibrium. Post-heating, lamps were removed to eliminate residual emission interference. Data processing focused on the cooling phase due to lamp reflection artifacts. The resulting thermal data cube consists of N time-resolved images (where N = cooling duration), analysable as individual frames or temperature profiles.

The acquired thermograms were processed by subtracting, on a pixel-by-pixel basis, the reference frame captured immediately before heating from all subsequent frames in the sequence.

C. LWIR Active Thermography

Long-wave infrared measurements employed a TESTO 890 thermal camera (8 – 14 µm, 1280 × 960 pixels, NETD < 40 mK, ± 2 °C accuracy from -30 °C to 100 °C, snapshot mode).

The experimental protocol (180 s heating with 1 kW lamps) and the data processing mirrored MWIR thermography, but thermal frames were acquired at variable time intervals, prioritizing higher sampling rates during early cooling for enhanced defect sensitivity.

D. THz Time–Domain Imaging

THz analysis was performed at CNR-IREA by means of a Menlo Systems TeraASOPS spectrometer, based on the Asynchronous Optical Sampling (ASOPS) principle [12]. The system has a nominal bandwidth (B) of 4 THz and a reference signal-to-noise ratio greater than 70 dB, which are achievable under operational conditions of 10 Hz laser difference frequency, 10 MHz sampling rate, 10^6 gain,

1000 waveform averages, and favourable environment conditions. The system collects signals within an observation time window (T_{max}) of 100 ps, which is movable across a 10 ns range. Accordingly, in the case of normal reflection measurements, the maximum depth that can be investigated is:

$$d_{max} = T_{max} \cdot \frac{v}{2} \quad (1)$$

v being the electromagnetic wav propagation velocity into the encountered materials. Note that d_{max} is always less than 1.5 cm. Moreover, when normal reflection data are gathered in uncontrolled environmental conditions, the actual frequency range is about 2 THz. Hence, the expected range resolution is about 100 µm in air.

The system is equipped with a motorised x-y scanner, which enables the THz probes to move automatically in front of the surface of the object being tested. The maximum scanned area is 30 × 30 cm^2, while the minimum spatial step is 100 µm.

To ensure that each section was properly aligned with respect to the THz probe, the entire sample was partitioned into nine areas according to the sample sections. Each area was scanned with a spatial offset of 0.5 mm. Hence, 2D THz images were obtained by plotting the maximum, the minimum, or the energy of the time-domain THz wave as collected at each measurement point.

IV. RESULTS

This study focuses on the most significant results from area 9, located in the lower right quadrant of the terracotta slab. The stratigraphy of this region consists of an underlying painted layer featuring three gold and silver leaf decorations, overlaid by a thin green *scialbo* wash (Fig. 2a,b). All applied techniques, whose technical specification are summarized in Table 1, successfully identified the subsurface metallic decorations, except for long-wave infrared (LWIR) thermography, which failed to resolve any sub-surface features (Fig. 2f). This limitation likely stems from the inherently low thermal emission signature of metal leaf within this spectral band.

Table 1. Technical specifications of the instruments used in this work.

	Vis-NIR scanner	MWIR camera	LWIR camera	THz spectrometer
Spectral range	395-2550 nm	3-5 µm	8-14 µm	0.15-3 mm
Pixel size	250 µm	/	/	0.5 mm
Image resolution	/	640 × 512 px	1280 × 960 px	/
Acquisition time	3 h for 1 m^2	Set by the user	Set by the user	1 h for 100 cm^2

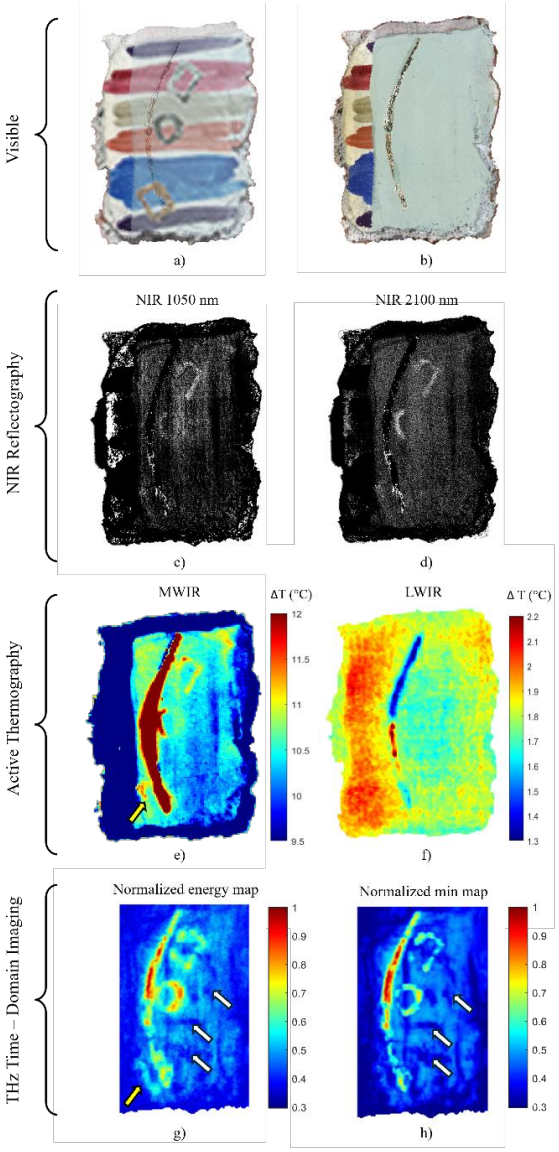

Fig. 2. a) Photograph captured during sample preparation, depicting the painted surface of area 9 with the green layer of scialbo, superimposed using the 60% layer opacity option; b) visible-light image of area 9. Imaging results of area 9: c),d) reflectance images at 1050 and 2100 nm, respectively; e), f) processed thermal images in the 3-5 µm and 8-14 µm spectral ranges, respectively; g), h) Normalised [0-1] energy and minimum maps of the THz signal.

Notable variations emerged in the techniques' detection capabilities regarding both the number of discernible decorations and the geometric precision of their outlines. NIR reflectography resolved only two of the three metallic elements, whereas MWIR thermography and THz imaging confirmed the presence of the third, inferiorly positioned decoration (denoted by yellow arrows in Fig. 2e,g). This detection discrepancy may arise from either the obscuring effect of overlying gold leaf or morphological

irregularities in the surface strata.

Further observational differences concern the central metallic motif, whose representation varied across techniques. While some modalities highlighted only the left portion (Fig. 2d,e), others emphasized the right sector (Fig. 2g). Such variations are attributable to microtopographic variations in surface relief.

Of note are the anomalous signals in THz imagery (white arrows in Fig. 2g,h), which exhibit no correlation with subsurface pigment distribution. These artifacts likely originate from superficial morphological features rather than stratigraphic discontinuities, underscoring the pronounced influence of surface topography on THz imaging outcomes.

V. CONCLUSIONS

This study employed a purpose-designed sample replicating mural painting stratigraphy, incorporating concealed decorative elements beneath surface layers, to evaluate a multi-technique imaging approach spanning near-infrared (NIR, 850 nm) to long-wave infrared (LWIR, 14 μm) and terahertz (THz) spectral ranges. The methodology integrated NIR reflectography, active thermography in both mid- and long- wave infrared (MWIR/LWIR), and THz Time-Domain imaging.

All the techniques successfully identified subsurface metallic decorations beneath thin *scialbo* layers irrespective of coloration, except for LWIR thermography, which proved ineffective due to the low thermal emissivity of metal leaf in this spectral region. However, none of the methods detected features obscured by plaster layers, as evidenced by the null results in area 4.

The experimental data demonstrated a pronounced correlation between the acquired signal and surface topography, with THz imaging exhibiting high sensitivity to superficial morphological variations. The multimodal analytical approach allowed for effective discrimination and mitigation of artefacts arising from surface morphology. To advance these findings, future work will involve high-resolution 3D surface modelling to establish a reference framework for signal interpretation, thereby enhancing the discriminative capacity of these diagnostic techniques.

ACKNOWLEDGMENTS

This research was funded by the project PNRR CHANGES (Cultural Heritage Active Innovation for Sustainable Society) Project (PE_00000020), CUP_D53C22002560006, funded by the European Union – Next Generation EU M4.C2.1.1 and PNRR H2IOSC (Humanities and Cultural Heritage ItalianOpen Science Cloud) Project (IR0000029), CUP_B63C22000730005, funded by Next Generation EU.

This research was also supported by the European Research Infrastructure for Heritage Science (E-RIHS), project CIR01_00016 SHINE.

We gratefully acknowledge the contribution of art conservator Ezio Buzzegoli in preparing the sample analysed in this research.

REFERENCES

[1] J. Striova, L. Pezzati, E. Pampaloni, R. Fontana, “Synchronized Hardware-Registered VIS-NIR Imaging Spectroscopy and 3D Sensing on a Fresco by Botticelli”, Sensors, vol.21, No.4, 2021, pp.1-14.

[2] S. Ceccarelli, N. Orazi, F. Mercuri, U. Zammit, S. Paoloni, “Mid-Wave Infrared Analysis of the Wall Drawing “Saint Joseph with the Child” by Gian Lorenzo Bernini”. In “Advanced Technologies for Cultural Heritage Monitoring and Conservation”, S. Ceccarelli, M. Missori, R. Fantoni, Eds.; Digital Innovations in Architecture, Engineering and Construction; Springer Nature Switzerland: Cham, 2024; pp.65–73.

[3] C. Daffara, S. Parisotto, P.I. Mariotti, D. Ambrosini, “Dual Mode Imaging in Mid Infrared with Thermal Signal Reconstruction for Innovative Diagnostics of the “Monocromo” by Leonardo Da Vinci”, Sci Rep, vol.11, No.1, 2021, pp.1-10.

[4] J.L. Bodnar, J.C. Candoré, J.L. Nicolas, G. Szatanik, V. Detalle, J.M. Vallet, “Stimulated Infrared Thermography Applied to Help Restoring Mural Paintings”, NDT & E International, vol.49, 2012, pp.40–46.

[5] J. Williams, F. Corvaro, J. Vignola, D. Turo, B. Marchetti, M. Vitali, “Application of Non-Invasive Active Infrared Thermography for Delamination Detection in Fresco”, International Journal of Thermal Sciences, vol.171, 2022, pp.1-13.

[6] C.L.K. Dandolo, P.U. Jepsen, “Wall Painting Investigation by Means of Non-Invasive Terahertz Time-Domain Imaging (THz-TDI): Inspection of Subsurface Structures Buried in Historical Plasters”. J Infrared Milli Terahz Waves, vol.37, No.2, 2016, pp.198–208.

[7] K. Fukunaga, “THz Technology Applied to Cultural Heritage in Practice”, Cultural Heritage Science, Springer, Tokyo, 2016.

[8] V. Di Sarno, S. Zappia, E. Vannini, A. Rocco, P. Maddaloni, R. Fontana, I. Catapano, “THz Time-Domain transmission and reflection imaging for art material analysis: preliminary results @E-RIHS.it”, 2025, Springer, in press.

[9] J. Hu, H. Zhang, S. Sfarra, G. Gargiulo, N.P. Avdelidis, M. Zhang, D. Yang, X. Maldague, “Non-Destructive Imaging of Marqueteries Based on a New Infrared-Terahertz Fusion Technique”, Infrared Physics & Technology, vol.125, 2022, pp.1-9.

[10] V. Tornari, M. Andrianakis, S. Duchêne, W. Nowik, D. Brissaud, D. Giovannacci, M. Küppers, C. Rehorn, B. Blümich, G. Ricci, G. Artioli, “A Combined ND Diagnostic Investigation by DHSPI, SIRT, NMR, THZ, on Giotto Fresco”, Journal of Cultural Heritage, vol.63, 2023, pp.206–216.

[11] C. Bonifazzi, P. Carcagnì, R. Fontana, M. Greco, M.

Mastroianni, M. Materazzi, E. Pampaloni, L. Pezzati, D. Bencini, “A Scanning Device for VIS–NIR Multispectral Imaging of Paintings”, Journal of Optics A Pure and Applied Optics, vol.10, No.6, 2008, pp.1-9.

[12] A. Bartels, R. Cerna, C. Kistner, A. Thoma, F. Hudert, C. Janke, T. Dekorsy, “Ultrafast Time-Domain Spectroscopy Based on High-Speed Asynchronous Optical Sampling”, Review of Scientific Instruments, vol.78, No.3, 2007, pp.1-8.